THE EUROPEAN
PHYSICAL JOURNAL C

Highly excited and exotic fully-strange tetraquark states

Rui-Rui Dong, Niu Su, Hua-Xing Chen[a]

School of Physics, Southeast University, Nanjing 210094, China

Abstract Some hadrons have the exotic quantum numbers that the traditional $\bar{q}q$ mesons and qqq baryons can not reach, such as $J^{PC} = 0^{--}/0^{+-}/1^{-+}/2^{+-}/3^{-+}/4^{+-}$, etc. We investigate for the first time the exotic quantum number $J^{PC} = 4^{+-}$, and study the fully-strange tetraquark states with such an exotic quantum number. We systematically construct all the diquark–antidiquark interpolating currents, and apply the method of QCD sum rules to calculate both the diagonal and off-diagonal correlation functions. The obtained results are used to construct three mixing currents that are nearly non-correlated, and we use one of them to extract the mass of the lowest-lying state to be $2.85^{+0.19}_{-0.22}$ GeV. We apply the Fierz rearrangement to transform this mixing current to be the combination of three meson–meson currents, and the obtained Fierz identity suggests that this state dominantly decays into the P-wave $\phi(1020) f_2'(1525)$ channel. This fully-strange tetraquark state of $J^{PC} = 4^{+-}$ is a purely exotic hadron to be potentially observed in future particle experiments.

1 Introduction

In the past twenty years many candidates of exotic hadrons were observed in particle experiments, which can not be well explained in the traditional quark model [1]. Most of them still have the "traditional" quantum numbers that the traditional $\bar{q}q$ mesons and qqq baryons can also reach, making them not so easy to be clearly identified as exotic hadrons. However, there are some "exotic" quantum numbers that the traditional hadrons can not reach, such as the spin-parity quantum numbers $J^{PC} = 0^{--}/0^{+-}/1^{-+}/2^{+-}/3^{-+}/4^{+-}/\cdots$. The hadrons with such

exotic quantum numbers are of particular interests, since they can not be explained as traditional hadrons any more. Their possible interpretations are compact multiquark states [2–5], hadronic molecules [6–8], glueballs [9–16], and hybrid states [17–26], etc.

Among these exotic quantum numbers, the states of $J^{PC} = 1^{-+}$ have been extensively studied in the literature [2,3,5–7,17–26], since they are predicted to be the lightest hybrid states [27]. Up to now there have been four structures observed in experiments with $J^{PC} = 1^{-+}$, including three isovector states $\pi_1(1400)$ [28], $\pi_1(1600)$ [29], and $\pi_1(2015)$ [30] as well as one isoscalar state $\eta_1(1855)$ [31]. Besides, the states of $J^{PC} = 0^{--}/0^{+-}/2^{+-}/3^{-+}$ have also been studied to some extent [4,8–16]. These theoretical and experimental studies have significantly improved our understanding on the non-perturbative behaviors of the strong interaction in the low energy region. However, there has not been any investigation on the exotic quantum number $J^{PC} = 4^{+-}$ yet.

In this paper we shall investigate for the first time the exotic quantum number $J^{PC} = 4^{+-}$, and study the fully-strange tetraquark states with such an exotic quantum number. We shall work within the diquark–antidiquark picture, and systematically construct all the diquark–antidiquark currents of $J^{PC} = 4^{+-}$, as depicted in Fig. 1a. We shall apply the method of QCD sum rules to study these currents as a whole, and extract the mass of the lowest-lying state to be $2.85^{+0.19}_{-0.22}$ GeV.

Besides, we shall also systematically construct all the meson–meson currents of $J^{PC} = 4^{+-}$, as depicted in Fig. 1b. We shall relate these currents and the diquark–antidiquark currents through the Fierz rearrangement. The obtained Fierz identity suggests that the lowest-lying state dominantly decays into the P-wave $\phi(1020) f_2'(1525)$ channel. Accordingly, we propose to search for it in the $X \rightarrow \phi(1020) f_2'(1525) \rightarrow \phi K\bar{K}$ decay process. With a large amount of J/ψ sample, the BESIII collaboration are intensively studying the physics happening around here. Such

R. Dong and N. Su equally contribute to this work.

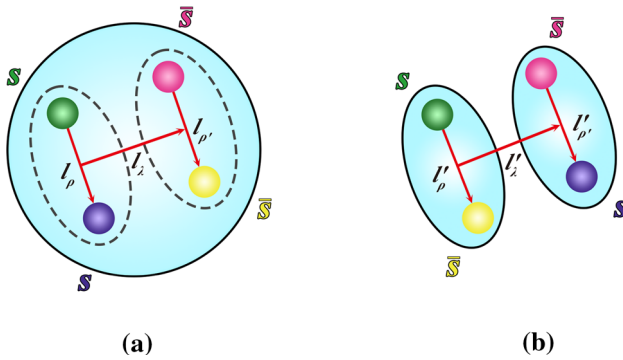[a] e-mail: hxchen@seu.edu.cn (corresponding author)

Fig. 1 Two configurations for the fully-strange tetraquark states: **a** the diquark–antidiquark system with the internal orbital angular momenta $l_\lambda/l_\rho/l_{\rho'}$ and **b** the meson–meson system with $l'_\lambda/l'_\rho/l'_{\rho'}$

experiments can also be performed by Belle-II, COMPASS, GlueX, and PANDA, etc. Accordingly, this fully-strange tetraquark state of $J^{PC} = 4^{+-}$ is a purely exotic hadron to be potentially observed in future particle experiments.

This paper is organized as follows. In Sect. 2 we systematically construct the local fully-strange tetraquark currents with the exotic quantum number $J^{PC} = 4^{+-}$. We use them to perform QCD sum rule analyses in Sect. 3, where we calculate both their diagonal and off-diagonal two-point correlation functions. Based on the obtained results, we use the three single currents to perform numerical analyses in Sect. 4, while their mixing currents are investigated in Sect. 5. Section 6 is a summary.

2 Fully-strange tetraquark currents

As the first step, we construct the local fully-strange tetraquark currents with the exotic quantum number $J^{PC} = 4^{+-}$. This quantum number can not be reached by simply using one quark and one antiquark, and moreover, we need two quarks and two antiquarks together with at least two derivatives to reach such a quantum number.

As depicted in Fig. 1, there are two possible configurations, the diquark–antidiquark configuration and the meson–meson configuration. When investigating the former configuration, the two covalent derivative operators $D_\alpha(\equiv \partial_\alpha + ig_s A_\alpha)$ and D_β can be either inside the diquark/antidiquark field or between them:

$$\eta = [s_a^T C \Gamma_1 \overset{\leftrightarrow}{D}_\alpha \overset{\leftrightarrow}{D}_\beta s_b](\bar{s}_c \Gamma_2 C \bar{s}_d^T) \pm h.c. ,$$
$$\eta' = [s_a^T C \Gamma_3 \overset{\leftrightarrow}{D}_\alpha s_b][\bar{s}_c \Gamma_4 C \overset{\leftrightarrow}{D}_\beta \bar{s}_d^T] \pm h.c. ,$$
$$\eta'' = [[s_a^T C \Gamma_5 \overset{\leftrightarrow}{D}_\alpha s_b] \overset{\leftrightarrow}{D}_\beta (\bar{s}_c \Gamma_6 C \bar{s}_d^T)] \pm h.c. ,$$
$$\eta''' = [(s_a^T C \Gamma_7 s_b) \overset{\leftrightarrow}{D}_\alpha \overset{\leftrightarrow}{D}_\beta (\bar{s}_c \Gamma_8 C \bar{s}_d^T)] \pm h.c. , \tag{1}$$

where $[A \overset{\leftrightarrow}{D}_\alpha B] \equiv A[D_\alpha B] - [D_\alpha A]B$, $a \cdots d$ are color

indices, and $\Gamma_{1\dots8}$ are Dirac matrices. The internal orbital angular momenta contained in these currents are

$$\eta : l_\lambda = 0, \ l_\rho = 2/0, \ l_{\rho'} = 0/2,$$
$$\eta' : l_\lambda = 0, \ l_\rho = 1, \ l_{\rho'} = 1,$$
$$\eta'' : l_\lambda = 1, \ l_\rho = 1/0, \ l_{\rho'} = 0/1,$$
$$\eta''' : l_\lambda = 2, \ l_\rho = 0, \ l_{\rho'} = 0. \tag{2}$$

After carefully examining all the possible combinations, we find that only the η currents can reach $J^{PC} = 4^{+-}$, as depicted in Fig. 2, while the $\eta'/\eta''/\eta'''$ currents can not. Altogether, we can construct three independent diquark–antidiquark currents of $J^{PC} = 4^{+-}$:

$$\eta^1_{\alpha_1\alpha_2\alpha_3\alpha_4} = \epsilon^{abe}\epsilon^{cde}$$
$$\times \mathcal{S}\Big\{[s_a^T C\gamma_{\alpha_1}\overset{\leftrightarrow}{D}_{\alpha_3}\overset{\leftrightarrow}{D}_{\alpha_4}s_b](\bar{s}_c\gamma_{\alpha_2}C\bar{s}_d^T)$$
$$- (s_a^T C\gamma_{\alpha_1}s_b)[\bar{s}_c\gamma_{\alpha_2}C\overset{\leftrightarrow}{D}_{\alpha_3}\overset{\leftrightarrow}{D}_{\alpha_4}\bar{s}_d^T]\Big\},$$
$$\eta^2_{\alpha_1\alpha_2\alpha_3\alpha_4} = (\delta^{ac}\delta^{bd} + \delta^{ad}\delta^{bc})$$
$$\times \mathcal{S}\Big\{[s_a^T C\gamma_{\alpha_1}\gamma_5\overset{\leftrightarrow}{D}_{\alpha_3}\overset{\leftrightarrow}{D}_{\alpha_4}s_b](\bar{s}_c\gamma_{\alpha_2}\gamma_5 C\bar{s}_d^T)$$
$$- (s_a^T C\gamma_{\alpha_1}\gamma_5 s_b)[\bar{s}_c\gamma_{\alpha_2}\gamma_5 C\overset{\leftrightarrow}{D}_{\alpha_3}\overset{\leftrightarrow}{D}_{\alpha_4}\bar{s}_d^T]\Big\},$$
$$\eta^3_{\alpha_1\alpha_2\alpha_3\alpha_4} = \epsilon^{abe}\epsilon^{cde}g^{\mu\nu}$$
$$\times \mathcal{S}\Big\{[s_a^T C\sigma_{\alpha_1\mu}\overset{\leftrightarrow}{D}_{\alpha_3}\overset{\leftrightarrow}{D}_{\alpha_4}s_b](\bar{s}_c\sigma_{\alpha_2\nu}C\bar{s}_d^T)$$
$$- (s_a^T C\sigma_{\alpha_1\mu}s_b)[\bar{s}_c\sigma_{\alpha_2\nu}C\overset{\leftrightarrow}{D}_{\alpha_3}\overset{\leftrightarrow}{D}_{\alpha_4}\bar{s}_d^T]\Big\}. \tag{3}$$

The symbol $\mathcal{S}$ denotes symmetrization and subtracting the trace terms in the set $\{\alpha_1 \cdots \alpha_J\}$. Among these currents, $\eta^1_{\dots}$ and $\eta^3_{\dots}$ have the antisymmetric color structure $[ss]_{\bar{3}_C}[\bar{s}\bar{s}]_{3_C}$, and $\eta^2_{\dots}$ has the symmetric color structure $[ss]_{6_C}[\bar{s}\bar{s}]_{\bar{6}_C}$.

After similarly investigating the meson–meson configuration, we can also construct three independent meson–meson currents of $J^{PC} = 4^{+-}$:

$$\xi^1_{\alpha_1\alpha_2\alpha_3\alpha_4} = \mathcal{S}\Big\{[\bar{s}_a\gamma_{\alpha_1}\overset{\leftrightarrow}{D}_{\alpha_3}s_a]\overset{\leftrightarrow}{D}_{\alpha_4}(\bar{s}_b\gamma_{\alpha_2}s_b)\Big\},$$
$$\xi^2_{\alpha_1\alpha_2\alpha_3\alpha_4} = \mathcal{S}\Big\{[\bar{s}_a\gamma_{\alpha_1}\gamma_5\overset{\leftrightarrow}{D}_{\alpha_3}s_a]\overset{\leftrightarrow}{D}_{\alpha_4}(\bar{s}_b\gamma_{\alpha_2}\gamma_5 s_b)\Big\},$$
$$\xi^3_{\alpha_1\alpha_2\alpha_3\alpha_4} = g^{\mu\nu}\mathcal{S}\Big\{[\bar{s}_a\sigma_{\alpha_1\mu}\overset{\leftrightarrow}{D}_{\alpha_3}s_a]\overset{\leftrightarrow}{D}_{\alpha_4}(\bar{s}_b\sigma_{\alpha_2\nu}s_b)\Big\}. \tag{4}$$

As depicted in Fig. 2, the internal orbital angular momenta contained in these currents are

$$\xi : l'_\lambda = 1, \ l'_\rho = 1, \ l'_{\rho'} = 0. \tag{5}$$

After applying the Fierz rearrangement, we obtain

$$\begin{pmatrix} \eta^1_{\dots} \\ \eta^2_{\dots} \\ \eta^3_{\dots} \end{pmatrix} = \begin{pmatrix} 2 & -2 & -2 \\ -2 & 2 & -2 \\ -4 & -4 & 0 \end{pmatrix} \begin{pmatrix} \xi^1_{\dots} \\ \xi^2_{\dots} \\ \xi^3_{\dots} \end{pmatrix}. \tag{6}$$

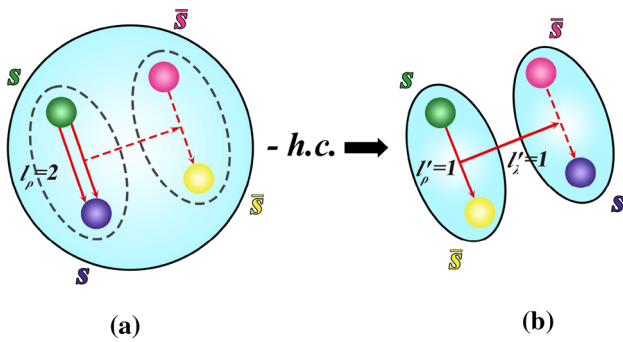This Fierz identity will be used to study the decay behaviors later.

Fig. 2 Possible internal orbital angular momenta contained in the fully-strange tetraquark currents of $J^{PC} = 4^{+-}$. The Fierz identity given in Eq. (6) indicates that the internal orbital angular momenta contained in the diquark–antidiquark system $\{l_\lambda = 0, l_\rho = 2/0, l_{\rho'} = 0/2\}$ correspond to those contained in the meson–meson system $\{l'_\lambda = 1, l'_\rho = 1, l'_{\rho'} = 0\}$

3 QCD sum rule analysis

We apply the QCD sum rule method [32,33] to study the fully-strange tetraquark currents $\eta^{1,2,3}_{\alpha_1\alpha_2\alpha_3\alpha_4}$ with the exotic quantum number $J^{PC} = 4^{+-}$. This non-perturbative method has been successfully applied to study various conventional and exotic hadrons in the past 50 years [34].

We generally assume that the current $\eta^i_{\alpha_1\alpha_2\alpha_3\alpha_4}$ ($i = 1\cdots3$) couples to the fully-strange tetraquark states X_n ($n = 1\cdots N$) through

$$\langle 0|\eta^i_{\alpha_1\alpha_2\alpha_3\alpha_4}|X_n\rangle = f_{in}\epsilon_{\alpha_1\alpha_2\alpha_3\alpha_4}, \quad (7)$$

where f_{in} is the $3 \times N$ matrix for the decay constants, and $\epsilon_{\alpha_1\alpha_2\alpha_3\alpha_4}$ is the traceless and symmetric polarization tensor satisfying

$$\epsilon_{\alpha_1\alpha_2\alpha_3\alpha_4}\epsilon^*_{\beta_1\beta_2\beta_3\beta_4} = \mathcal{S}'[\tilde{g}_{\alpha_1\beta_1}\tilde{g}_{\alpha_2\beta_2}\tilde{g}_{\alpha_3\beta_3}\tilde{g}_{\alpha_4\beta_4}], \quad (8)$$

with $\tilde{g}_{\mu\nu} = g_{\mu\nu} - q_\mu q_\nu/q^2$. The symbol $\mathcal{S}'$ denotes symmetrization and subtracting the trace terms in the sets $\{\alpha_1\alpha_2\alpha_3\alpha_4\}$ and $\{\beta_1\beta_2\beta_3\beta_4\}$.

Based on Eq. (7), we can investigate both the diagonal and off-diagonal correlation functions:

$$\Pi^{ij}_{\alpha_1\alpha_2\alpha_3\alpha_4;\beta_1\beta_2\beta_3\beta_4}(q^2)$$
$$\equiv i \int d^4x e^{iqx}\langle 0|\mathbf{T}[\eta^i_{\alpha_1\alpha_2\alpha_3\alpha_4}(x)\eta^{j,\dagger}_{\beta_1\beta_2\beta_3\beta_4}(0)]|0\rangle$$
$$= \Pi_{ij}(q^2) \times \mathcal{S}'[\tilde{g}_{\alpha_1\beta_1}\tilde{g}_{\alpha_2\beta_2}\tilde{g}_{\alpha_3\beta_3}\tilde{g}_{\alpha_4\beta_4}]. \quad (9)$$

At the hadron level we express $\Pi_{ij}(q^2)$ using the dispersion relation as

$$\Pi_{ij}(q^2) = \int_{s_<}^{\infty} \frac{\rho^{\text{phen}}_{ij}(s)}{s - q^2 - i\varepsilon}ds, \quad (10)$$

with $s_< = 16m_s^2$ the physical threshold. We parameterize the spectral density $\rho^{\text{phen}}_{ij}(s)$ for the states X_n together with

a continuum contribution as

$$\rho^{\text{phen}}_{ij}(s) \times \mathcal{S}'[\cdots]$$
$$\equiv \sum_n \delta(s - M_n^2)\langle 0|\eta^i_{...}|n\rangle\langle n|\eta^{j,\dagger}_{...}|0\rangle + \cdots$$
$$= \sum_n f_{in}f_{jn}\delta(s - M_n^2) \times \mathcal{S}'[\cdots] + \cdots, \quad (11)$$

with M_n the mass of X_n.

At the quark–gluon level we calculate $\Pi_{ij}(q^2)$ using the method of operator product expansion (OPE), and extract the OPE spectral density $\rho_{ij}(s) \equiv \rho^{\text{OPE}}_{ij}(s)$ [35]. In the calculations we take into account the Feynman diagrams depicted in Fig. 3. We consider the perturbative term, the strange quark mass m_s, the quark condensate $\langle\bar{s}s\rangle$, the quark–gluon mixed condensate $\langle g_s\bar{s}\sigma Gs\rangle$, the gluon condensate $\langle g_s^2GG\rangle$, and their combinations. We calculate all the diagrams proportional to $g_s^{N=0}$ and $g_s^{N=1}$, where we find the $D = 6$ term $\langle\bar{s}s\rangle^2$ and the $D = 8$ term $\langle\bar{s}s\rangle\langle g_s\bar{s}\sigma Gs\rangle$ to be important. We partly calculate the diagrams proportional to $g_s^{N\geq2}$, whose contributions are found to be small. Especially, we have not taken into account the radiative corrections in our QCD sum rule calculations.

Then we perform the Borel transformation at both the hadron and quark–gluon levels. After approximating the continuum using $\rho_{ij}(s)$ above the threshold value s_0, we obtain the sum rule equation

$$\Pi_{ij}(s_0, M_B^2) \equiv \sum_n f_{in}f_{jn}e^{-M_n^2/M_B^2}$$
$$= \int_{s_<}^{s_0} e^{-s/M_B^2}\rho_{ij}(s)ds. \quad (12)$$

We shall investigate it through two steps, the single-channel analysis and the multi-channel analysis, as follows.

4 Single-channel analysis

To perform the single-channel analysis, we neglect the off-diagonal correlation functions by setting $\rho_{ij}(s)|_{i\neq j} = 0$ so that only $\rho_{ii}(s) \neq 0$. This assumption means that the three currents $\eta^{1,2,3}_{\alpha_1\alpha_2\alpha_3\alpha_4}$ are "non-correlated", and any two of them can not mainly couple to the same state X, otherwise,

$$\rho_{ij}(s) \times \mathcal{S}'[\cdots]$$
$$\equiv \sum_n \delta(s - M_n^2)\langle 0|\eta^i_{...}|n\rangle\langle n|\eta^{j,\dagger}_{...}|0\rangle + \cdots$$
$$\approx \delta(s - M_X^2)\langle 0|\eta^i_{...}|X\rangle\langle X|\eta^{j,\dagger}_{...}|0\rangle + \cdots$$
$$\neq 0. \quad (13)$$

Accordingly, we assume that there are three states $X_{1,2,3}$ corresponding to the three currents $\eta^{1,2,3}_{\alpha_1\alpha_2\alpha_3\alpha_4}$ through

$$\langle 0|\eta^i_{\alpha_1\alpha_2\alpha_3\alpha_4}|X_i\rangle = f_{ii}\epsilon_{\alpha_1\alpha_2\alpha_3\alpha_4}. \quad (14)$$
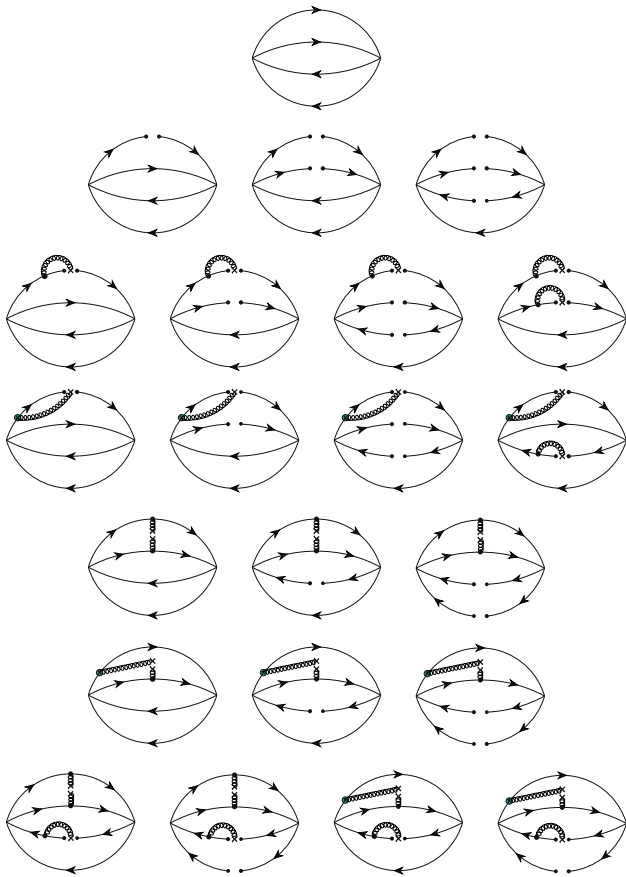
Fig. 3 Feynman diagrams for the fully-strange tetraquark currents of $J^{PC} = 4^{+-}$. The covariant derivative operator $D_\alpha = \partial_\alpha + i g_s A_\alpha$ contains two terms, and we depict the latter term using a green vertex

After parameterizing the spectral density $\rho_{ii}(s)$ as one pole dominance for the state X_i together with a continuum contribution, Eq. (12) is simplified to be

$$\Pi_{ii}(s_0, M_B^2) \equiv f_{ii}^2 e^{-M_i^2/M_B^2} = \int_{s_<}^{s_0} e^{-s/M_B^2} \rho_{ii}(s) ds, \quad (15)$$

which can be used to calculate M_i through

$$M_i^2(s_0, M_B) = \frac{\int_{s_<}^{s_0} e^{-s/M_B^2} s \rho_{ii}(s) ds}{\int_{s_<}^{s_0} e^{-s/M_B^2} \rho_{ii}(s) ds}. \quad (16)$$

We use the spectral density $\rho_{11}(s)$ extracted from the current $\eta_{\alpha_1\alpha_2\alpha_3\alpha_4}^1$ as an example to perform the numerical analysis. We take the following values for various QCD parameters [1,36–42]:

$$m_s(2 \text{ GeV}) = 93_{-5}^{+11} \text{ MeV},$$
$$\left\langle g_s^2 GG \right\rangle = (0.48 \pm 0.14) \text{ GeV}^4,$$
$$\langle \bar{s}s \rangle = -(0.8 \pm 0.1) \times (0.240 \text{ GeV})^3,$$
$$\langle g_s \bar{s} \sigma G s \rangle = -M_0^2 \times \langle \bar{s}s \rangle,$$
$$M_0^2 = (0.8 \pm 0.2) \text{ GeV}^2. \quad (17)$$

As shown in Eq. (16), the mass M_1 of the state X_1 depends on two free parameters, the Borel mass M_B and the threshold value s_0. We investigate three aspects to find their proper working regions: (a) the convergence of OPE, (b) the sufficient amount of the pole contribution, and (c) the mass dependence on these two parameters.

Firstly, we investigate the convergence of OPE, which is the cornerstone for a reliable QCD sum rule analysis. We require the $D = 12$ terms (CVG$_{12}$) to be less than 5%, the $D = 10$ terms (CVG$_{10}$) to be less than 10%, and the $D = 8$ terms (CVG$_8$) to be less than 20%:

$$\text{CVG}_{12} \equiv \left| \frac{\Pi_{11}^{D=12}(\infty, M_B^2)}{\Pi_{11}(\infty, M_B^2)} \right| < 5\%, \quad (18)$$

$$\text{CVG}_{10} \equiv \left| \frac{\Pi_{11}^{D=10}(\infty, M_B^2)}{\Pi_{11}(\infty, M_B^2)} \right| < 10\%, \quad (19)$$

$$\text{CVG}_8 \equiv \left| \frac{\Pi_{11}^{D=8}(\infty, M_B^2)}{\Pi_{11}(\infty, M_B^2)} \right| < 20\%. \quad (20)$$

As depicted in Fig. 4 using the dashed curves, the lower bound of the Borel mass is determined to be $M_B^2 > 2.40 \text{ GeV}^2$.

Secondly, we investigate the one-pole-dominance assumption by requiring the pole contribution (PC) to be larger than 40%:

$$\text{PC} \equiv \left| \frac{\Pi_{11}(s_0, M_B^2)}{\Pi_{11}(\infty, M_B^2)} \right| > 40\%. \quad (21)$$

As depicted in Fig. 4 using the solid curve, the upper bound of the Borel mass is determined to be $M_B^2 < 2.65 \text{ GeV}^2$ when setting $s_0 = 16.0 \text{ GeV}^2$. Altogether the Borel window is determined to be $2.40 \text{ GeV}^2 < M_B^2 < 2.65 \text{ GeV}^2$ for $s_0 = 16.0 \text{ GeV}^2$. Redoing the same procedures, we find that there are non-vanishing Borel windows for $s_0 > s_0^{\min} = 14.6 \text{ GeV}^2$. Accordingly, we choose s_0 to be slightly larger,
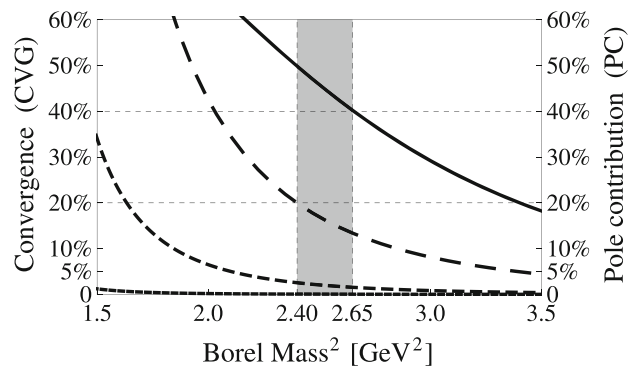

Fig. 4 CVG$_{12}$ (short-dashed curve, defined in Eq. (18)), CVG$_{10}$ (middle-dashed curve, defined in Eq. (19)), CVG$_8$ (long-dashed curve, defined in Eq. (20)), and PC (solid curve, defined in Eq. (21)) as functions of the Borel mass M_B. These curves are obtained using the current $\eta_{\alpha_1\alpha_2\alpha_3\alpha_4}^1$ when setting $s_0 = 16.0 \text{ GeV}^2$

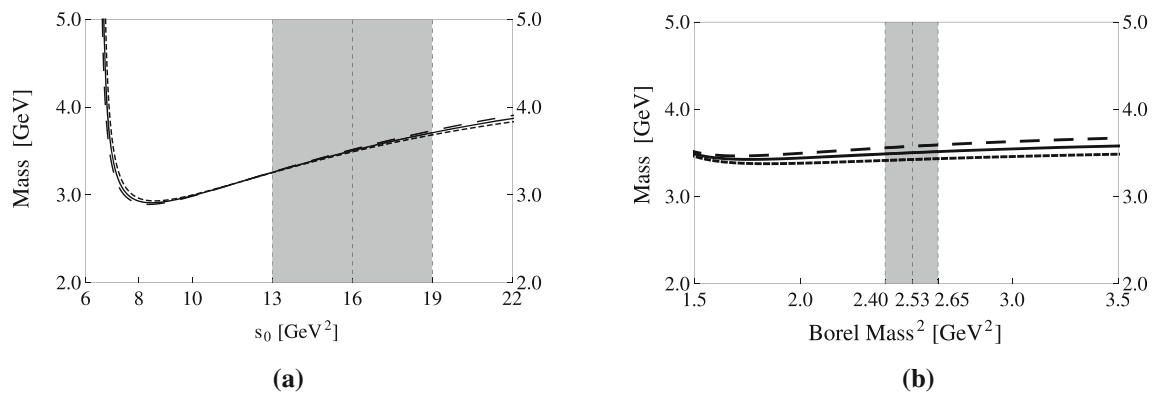**(a)**

(b)

Fig. 5 The mass M_1 of the state X_1 extracted from the current $\eta^1_{\alpha_1\alpha_2\alpha_3\alpha_4}$, with respect to **a** the threshold value s_0 and **b** the Borel mass M_B: **a** the short-dashed/solid/long-dashed curves are obtained by setting $M_B^2 = 2.40/2.53/2.65$ GeV^2, respectively; **b** the short-dashed/solid/long-dashed curves are obtained by setting $s_0 = 15.0/16.0/17.0$ GeV^2, respectively

Table 1 QCD sum rule results for the fully-strange tetraquark states with the exotic quantum number $J^{PC} = 4^{+-}$, extracted from the diquark–antidiquark currents $\eta^{1,2,3}_{\alpha_1\alpha_2\alpha_3\alpha_4}$ as well as their mixing currents $J^{1,2,3}_{\alpha_1\alpha_2\alpha_3\alpha_4}$

Currents	s_0^{min} [GeV^2]	Working regions		Pole [%]	Mass [GeV]
		M_B^2 [GeV^2]	s_0 [GeV^2]		
$\eta^1_{\alpha_1\alpha_2\alpha_3\alpha_4}$	14.6	2.40–2.65	16 ± 3.0	40–50	$3.50^{+0.21}_{-0.25}$
$\eta^2_{\alpha_1\alpha_2\alpha_3\alpha_4}$	19.2	2.80–3.13	21 ± 4.0	40–51	$4.08^{+0.26}_{-0.31}$
$\eta^3_{\alpha_1\alpha_2\alpha_3\alpha_4}$	11.0	1.25–1.65	12 ± 2.0	40–58	$3.34^{+0.39}_{-0.18}$
$J^1_{\alpha_1\alpha_2\alpha_3\alpha_4}$	10.1	1.78–1.92	11 ± 2.0	40–48	$2.85^{+0.19}_{-0.22}$
$J^2_{\alpha_1\alpha_2\alpha_3\alpha_4}$	19.1	2.79–3.14	21 ± 4.0	40–51	$4.08^{+0.26}_{-0.31}$
$J^3_{\alpha_1\alpha_2\alpha_3\alpha_4}$	–	–	–	–	–

and determine its working region to be 13.0 GeV$^2 < s_0 <$ 19.0 GeV^2.

Thirdly, we show the mass M_1 in Fig. 5, and investigate its dependence on M_B and s_0. It is stable against M_B inside the Borel window 2.40 GeV$^2 < M_B^2 <$ 2.65 GeV^2, and its dependence on s_0 is moderate insider the working region 13.0 GeV$^2 < s_0 <$ 19.0 GeV^2, where the mass is calculated to be

$$M_1 = 3.50^{+0.21}_{-0.25} \text{ GeV}. \tag{22}$$

Its uncertainty is due to s_0 and M_B as well as various QCD parameters listed in Eq. (17).

We repeat the same procedures to study the other two currents $\eta^2_{\alpha_1\alpha_2\alpha_3\alpha_4}$ and $\eta^3_{\alpha_1\alpha_2\alpha_3\alpha_4}$. The obtained results are summarized in Table 1.

5 Multi-channel analysis

To perform the multi-channel analysis, we take into account the off-diagonal correlation functions, which are actually non-zero, i.e., $\rho_{ij}(s)|_{i \neq j} \neq 0$. It is interesting to see how

large they are, so we choose $s_0 = 11.0$ GeV^2 and $M_B^2 = 1.85$ GeV^2 to obtain

$$\Pi_{ij}(s_0, M_B^2) = \begin{pmatrix} 2.77 & -0.04 & -3.83 \\ -0.04 & 0.98 & 0.46 \\ -3.83 & 0.46 & 2.38 \end{pmatrix} \times 10^{-6} \text{ GeV}^{14}. \tag{23}$$

Hence, $\eta^1_{...}$ and $\eta^3_{...}$ are strongly correlated with each other, making the off-diagonal terms of $\rho_{ij}(s)$ non-negligible, as depicted in Fig. 6 using the solid curve.

To diagonalize the 3×3 matrix $\rho_{ij}(s)$, we construct three mixing currents $J^{1,2,3}_{\alpha_1\alpha_2\alpha_3\alpha_4}$:

$$\begin{pmatrix} J^1_{...} \\ J^2_{...} \\ J^3_{...} \end{pmatrix} = \mathbb{T}_{3 \times 3} \begin{pmatrix} \eta^1_{...} \\ \eta^2_{...} \\ \eta^3_{...} \end{pmatrix}, \tag{24}$$

with $\mathbb{T}_{3 \times 3}$ the transition matrix.

We apply the method of operator product expansion to extract the spectral densities $\rho'_{ij}(s)$ from the mixing currents $J^{1,2,3}_{\alpha_1\alpha_2\alpha_3\alpha_4}$. After choosing
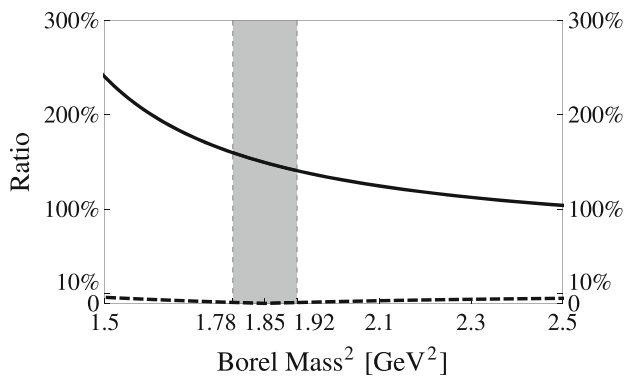
Fig. 6 Off-diagonal terms, $\left|\Pi_{13}/\sqrt{\Pi_{11}\Pi_{33}}\right|$ (solid) and $\left|\Pi'_{13}/\sqrt{\Pi'_{11}\Pi'_{33}}\right|$ (dashed), as functions of the Borel mass M_B. These curves are obtained by setting $s_0 = 11.0$ GeV^2

$$\mathbb{T}_{3\times3} = \begin{pmatrix} 0.72 & -0.06 & -0.69 \\ 0.14 & 0.99 & 0.05 \\ 0.68 & -0.13 & 0.72 \end{pmatrix}, \quad (25)$$

we obtain

$$\Pi'_{ij}(s_0, M_B^2) = \begin{pmatrix} 6.43 & 0 & 0 \\ 0 & 1.00 & 0 \\ 0 & 0 & -1.30 \end{pmatrix} \times 10^{-6} \text{ GeV}^{14}, \quad (26)$$

at $s_0 = 11.0$ GeV^2 and $M_B^2 = 1.85$ GeV^2. Hence, the off-diagonal terms of $\rho'_{ij}(s)$ are negligible around here, suggesting that the three mixing currents $J^{1,2,3}_{\alpha_1\alpha_2\alpha_3\alpha_4}$ are nearly non-correlated around here, as depicted in Fig. 6 using the dashed curve. Moreover, Eq. (26) indicates that the QCD sum rule result from $J^3_{\alpha_1\alpha_2\alpha_3\alpha_4}$ is non-physical around here due to its negative correlation function. Besides, Eq. (25) indicates that $J^2_{...}$ is almost the same as $\eta^2_{...}$, while $J^1_{...}$ and $J^3_{...}$ are mainly from the recombination of $\eta^1_{...}$ and $\eta^3_{...}$.

We use the procedures previously applied on the diquark–antidiquark currents $\eta^{1,2,3}_{\alpha_1\alpha_2\alpha_3\alpha_4}$ to study their mixing cur-

rents $J^{1,2,3}_{\alpha_1\alpha_2\alpha_3\alpha_4}$. The obtained results are also summarized in Table 1. Especially, the mass extracted from the current $J^1_{\alpha_1\alpha_2\alpha_3\alpha_4}$ is significantly reduced to be

$$M'_1 = 2.85^{+0.19}_{-0.22} \text{ GeV}. \quad (27)$$

For completeness, we show it in Fig. 7 as a function of the threshold value s_0 and the Borel mass M_B.

6 Conclusion

In this paper we apply the method of QCD sum rules to study the fully-strange tetraquark states with the exotic quantum number $J^{PC} = 4^{+-}$. We work within the diquark–antidiquark picture and systematically construct their interpolating currents. We calculate both the diagonal and off-diagonal correlation functions. The obtained results are used to construct three mixing currents that are nearly non-correlated. We use the mixing current $J^1_{\alpha_1\alpha_2\alpha_3\alpha_4}$ to evaluate the mass of the lowest-lying state to be $2.85^{+0.19}_{-0.22}$ GeV.

In this paper we also systematically construct the fully-strange meson–meson currents of $J^{PC} = 4^{+-}$, and relate them to the diquark–antidiquark currents through the Fierz rearrangement. Especially, we can apply Eqs. (24) and (6) to transform the mixing current $J^1_{\alpha_1\alpha_2\alpha_3\alpha_4}$ to be

$$J^1_{...} = 4.3\,\xi^1_{...} + 1.2\,\xi^2_{...} - 1.3\,\xi^3_{...}. \quad (28)$$

This Fierz identity suggests that the lowest-lying state dominantly decays into the P-wave $\phi(1020)f'_2(1525)$ channel through the meson–meson current $\xi^1_{\alpha_1\alpha_2\alpha_3\alpha_4}$, given that the operator $\bar{s}_b\gamma_{\alpha_2}s_b$ of $I^G J^{PC} = 0^-1^{--}$ well couples to the vector meson $\phi(1020)$ and the operator $\mathcal{S}[\bar{s}_a\gamma_{\alpha_1}\overleftrightarrow{D}_{\alpha_3}s_a]$ of $I^G J^{PC} = 0^+2^{++}$ well couples to the $f'_2(1525)$ meson. Accordingly, we propose to search for it in the $X \rightarrow \phi(1020)f'_2(1525) \rightarrow \phi K\bar{K}$ decay process in the future
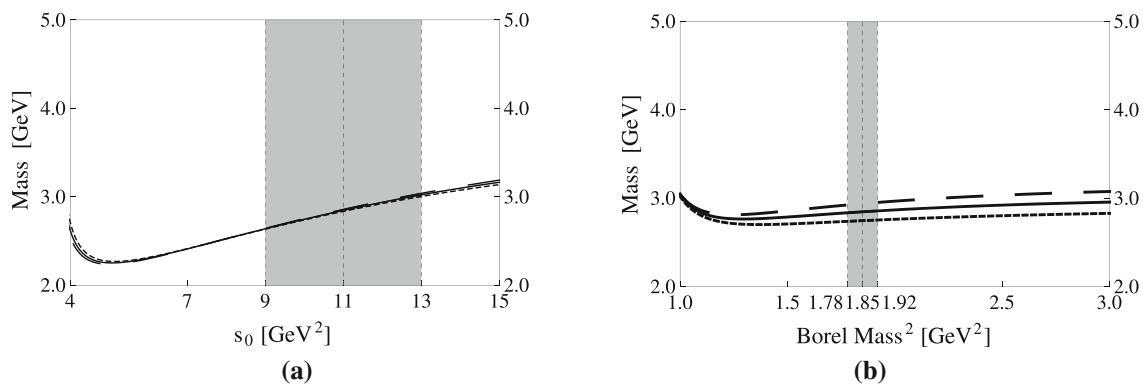

Fig. 7 The mass M'_1 extracted from the mixing current $J^1_{\alpha_1\alpha_2\alpha_3\alpha_4}$, with respect to **a** the threshold value s_0 and **b** the Borel mass M_B: **a** the short-dashed/solid/long-dashed curves are obtained by setting $M_B^2 =$ 1.78/1.85/1.92 GeV^2, respectively; **b** the short-dashed/solid/long-dashed curves are obtained by setting $s_0 = 10.0/11.0/12.0$ GeV^2, respectively

Belle-II, BESIII, COMPASS, GlueX, and PANDA experiments.

This is the first study on the exotic quantum number $J^{PC} = 4^{+-}$, and the above lowest-lying fully-strange tetraquark state of $J^{PC} = 4^{+-}$ is a purely exotic hadron to be potentially observed in future experiments. Its theoretical and experimental studies will continuously improve our understanding on the non-perturbative behaviors of the strong interaction in the low energy region.

Data Availability Statement This manuscript has data included as electronic supplementary material. The online version of this article contains supplementary material, which is available to authorized users.

References

1. P.A. Zyla et al. [Particle Data Group], Review of Particle Physics. PTEP **2020**, 083C01 (2020). https://doi.org/10.1093/ptep/ptaa104
2. H.X. Chen, A. Hosaka, S.L. Zhu, $I^G J^{PC} = 1^- 1^{-+}$ tetraquark states. Phys. Rev. D **78**, 054017 (2008). https://doi.org/10.1103/PhysRevD.78.054017
3. H.X. Chen, A. Hosaka, S.L. Zhu, $I^G J^{PC} = 0^+ 1^{-+}$ tetraquark state. Phys. Rev. D **78**, 117502 (2008). https://doi.org/10.1103/PhysRevD.78.117502
4. W. Zhu, Y.R. Liu, T. Yao, Is $J^{PC} = 3^{-+}$ molecule possible? Chin. Phys. C **39**, 023101 (2015). https://doi.org/10.1088/1674-1137/39/2/023101
5. Z.R. Huang, W. Chen, T.G. Steele, Z.F. Zhang, H.Y. Jin, Investigation of the light four-quark states with exotic $J^{PC} = 0^-$. Phys. Rev. D **95**, 076017 (2017). https://doi.org/10.1103/PhysRevD.95.076017
6. X. Zhang, J.J. Xie, Prediction of possible exotic states in the $\eta \bar{K} K^*$ system. Chin. Phys. C **44**, 054104 (2020). https://doi.org/10.1088/1674-1137/44/5/054104
7. X.K. Dong, Y.H. Lin, B.S. Zou, Interpretation of the $\eta_1(1855)$ as a $K \bar{K}_1(1400) + c.c.$ molecule. Sci. China Phys. Mech. Astron. **65**, 261011 (2022). https://doi.org/10.1007/s11433-022-1887-5
8. T. Ji, X.K. Dong, F.K. Guo, B.S. Zou, Prediction of a narrow exotic hadronic state with quantum numbers $J^{PC} = 0^-$.

9. C.J. Morningstar, M.J. Peardon, The Glueball spectrum from an anisotropic lattice study. Phys. Rev. D **60**, 034509 (1999). https://doi.org/10.1103/PhysRevD.60.034509
10. Y. Chen et al., Glueball spectrum and matrix elements on anisotropic lattices. Phys. Rev. D **73**, 014516 (2006). https://doi.org/10.1103/PhysRevD.73.014516
11. V. Mathieu, N. Kochelev, V. Vento, The physics of glueballs. Int. J. Mod. Phys. E **18**, 1 (2009). https://doi.org/10.1142/S0218301309012124
12. H.B. Meyer, Glueball regge trajectories. arXiv:hep-lat/0508002
13. E. Gregory, A. Irving, B. Lucini, C. McNeile, A. Rago, C. Richards, E. Rinaldi, Towards the glueball spectrum from unquenched lattice QCD. JHEP **1210**, 170 (2012). https://doi.org/10.1007/JHEP10(2012)170
14. A. Athenodorou, M. Teper, The glueball spectrum of SU(3) gauge theory in 3 + 1 dimensions. JHEP **11**, 172 (2020). https://doi.org/10.1007/JHEP11(2020)172
15. C.F. Qiao, L. Tang, Finding the 0^- glueball. Phys. Rev. Lett. **113**, 221601 (2014). https://doi.org/10.1103/PhysRevLett.113.221601
16. A. Pimikov, H.J. Lee, N. Kochelev, P. Zhang, V. Khandramai, Exotic glueball $0^{\pm-}$ states in QCD sum rules. Phys. Rev. D **96**, 114024 (2017). https://doi.org/10.1103/PhysRevD.96.114024
17. J.M. Frere, S. Titard, A new look at exotic decays: $\tilde{\rho}(1^{-+}, I = 1) \to \eta'\pi$ versus $\rho\pi$. Phys. Lett. B **214**, 463–466 (1988). https://doi.org/10.1016/0370-2693(88)91395-0
18. P.R. Page, E.S. Swanson, A.P. Szczepaniak, Hybrid meson decay phenomenology. Phys. Rev. D **59**, 034016 (1999). https://doi.org/10.1103/PhysRevD.59.034016
19. C.W. Bernard et al., [MILC Collaboration], Exotic mesons in quenched lattice QCD. Phys. Rev. D **56**, 7039–7051 (1997). https://doi.org/10.1103/PhysRevD.56.7039
20. J.J. Dudek, R.G. Edwards, M.J. Peardon, D.G. Richards, C.E. Thomas, Highly excited and exotic meson spectrum from dynamical lattice QCD. Phys. Rev. Lett. **103**, 262001 (2009). https://doi.org/10.1103/PhysRevLett.103.262001
21. J.J. Dudek et al., [Hadron Spectrum Collaboration], Toward the excited isoscalar meson spectrum from lattice QCD. Phys. Rev. D **88**, 094505 (2013). https://doi.org/10.1103/PhysRevD.88.094505
22. K.G. Chetyrkin, S. Narison, Light hybrid mesons in QCD. Phys. Lett. B **485**, 145 (2000). https://doi.org/10.1016/S0370-2693(00)00621-3
23. H.X. Chen, Z.X. Cai, P.Z. Huang, S.L. Zhu, Decay properties of the 1^{-+} hybrid state. Phys. Rev. D **83**, 014006 (2011). https://doi.org/10.1103/PhysRevD.83.014006
24. Z.R. Huang, H.Y. Jin, T.G. Steele, Z.F. Zhang, Revisiting the $b_1\pi$ and $\rho\pi$ decay modes of the 1^{-+} light hybrid state with light-cone QCD sum rules. Phys. Rev. D **94**, 054037 (2016). https://doi.org/10.1103/PhysRevD.94.054037
25. L. Qiu, Q. Zhao, Towards the establishment of the light $J^{P(C)} = 1^{-(+)}$ hybrid nonet. Chin. Phys. C **46**, 051001 (2022). https://doi.org/10.1088/1674-1137/ac567e
26. X.Y. Wang, F.C. Zeng, X. Liu, Production of the $\eta_1(1855)$ through kaon induced reactions under the assumptions that it is a molecular or a hybrid state. Phys. Rev. D **106**(3), 036005 (2022). https://doi.org/10.1103/PhysRevD.106.036005
27. C.A. Meyer, E.S. Swanson, Hybrid mesons. Prog. Part. Nucl. Phys. **82**, 21–58 (2015). https://doi.org/10.1016/j.ppnp.2015.03.001
28. D. Alde et al., [LAPP Collaboration], Evidence for a 1^{-+} Exotic Meson. Phys. Lett. B **205**, 397 (1988). https://doi.org/10.1016/0370-2693(88)91686-3
29. G.S. Adams et al., [E852 Collaboration], Observation of a new $J^{PC} = 1^{-+}$ exotic state in the reaction $\pi^- p \to \pi^+\pi^-\pi^- p$ at 18 GeV/c. Phys. Rev. Lett. **81**, 5760–5763 (1998). https://doi.org/10.1103/PhysRevLett.81.5760

30. J. Kuhn et al., [E852 Collaboration], Exotic meson production in the $f_1(1285)\pi^-$ system observed in the reaction $\pi^- p \to \eta\pi^+\pi^-\pi^- p$ at 18 GeV/c. Phys. Lett. B **595**, 109–117 (2004). https://doi.org/10.1016/j.physletb.2004.05.032

31. M. Ablikim et al., [BESIII Collaboration], Observation of an isoscalar resonance with exotic $J^{PC} = 1^{-+}$ quantum numbers in $J/\psi \to \gamma\eta\eta'$. arXiv:2202.00621 [hep-ex]

32. M.A. Shifman, A.I. Vainshtein, V.I. Zakharov, QCD and resonance physics. Theoretical foundations. Nucl. Phys. B **147**, 385 (1979). https://doi.org/10.1016/0550-3213(79)90022-1

33. L.J. Reinders, H. Rubinstein, S. Yazaki, Hadron properties from QCD sum rules. Phys. Rep. **127**, 1 (1985). https://doi.org/10.1016/0370-1573(85)90065-1

34. M. Nielsen, F.S. Navarra, S.H. Lee, New charmonium states in QCD sum rules: a concise review. Phys. Rep. **497**, 41–83 (2010). https://doi.org/10.1016/j.physrep.2010.07.005

35. All the spectral densities calculated in the present study are given in the supplementary file "OPE.nb"

36. K.C. Yang, W.Y.P. Hwang, E.M. Henley, L.S. Kisslinger, QCD sum rules and neutron proton mass difference. Phys. Rev. D **47**, 3001–3012 (1993). https://doi.org/10.1103/PhysRevD.47.3001

37. S. Narison, QCD as a theory of hadrons (from partons to confinement). Camb. Monogr. Part. Phys. Nucl. Phys. Cosmol. **17**, 1 (2002)

38. V. Gimenez, V. Lubicz, F. Mescia, V. Porretti, J. Reyes, Operator product expansion and quark condensate from lattice QCD in coordinate space. Eur. Phys. J. C **41**, 535–544 (2005). https://doi.org/10.1140/epjc/s2005-02250-9

39. M. Jamin, Flavor-symmetry breaking of the quark condensate and chiral corrections to the Gell–Mann–Oakes–Renner relation. Phys. Lett. B **538**, 71–76 (2002). https://doi.org/10.1016/S0370-2693(02)01951-2

40. B.L. Ioffe, K.N. Zyablyuk, Gluon condensate in charmonium sum rules with three-loop corrections. Eur. Phys. J. C **27**, 229–241 (2003). https://doi.org/10.1140/epjc/s2002-01099-8

41. A.A. Ovchinnikov, A.A. Pivovarov, QCD sum rule calculation of the quark gluon condensate. Sov. J. Nucl. Phys. **48**, 721 (1988)

42. J.R. Ellis, E. Gardi, M. Karliner, M.A. Samuel, Renormalization scheme dependence of Pade summation in QCD. Phys. Rev. D **54**, 6986–6996 (1996). https://doi.org/10.1103/PhysRevD.54.6986